

Assessment of Safe Loading Conditions for the SPCB Deck Crane Using Hydrostatic and GZ Curve Analysis

Budhi Santoso¹, Romadhoni¹, Polaris Nasution², Hardiyanto³, Zulfaidah Ariany⁴

(Received: 19 May 2025 / Revised: 27 May 2025 / Accepted: 3 June 2025 / Available Online: 30 June 2025)

Abstract—Heavy-lift deck cranes mounted on self-propelled crane barges (SPCB) can seriously erode transverse stability when large loads are handled at long outreach, yet clear, quantitative limits for operators are still scarce. This study therefore seeks to establish safe loading envelopes for an SPCB deck crane by combining standard hydrostatic calculations with complete righting-arm (GZ) curve analysis. Hydrostatic parameters were recomputed for four representative conditions—lightship, full ballast, maximum crane outreach, and uneven cargo stowage—using data from the vessel's stability booklet, and the resulting GZ curves were checked against SOLAS/IACS intact-stability criteria. Filling the ballast tanks raised the metacentric height (GM) to roughly 1.5 m and the area under the GZ curve (AUC) to 1.15 m·rad, offering the greatest safety margin; in contrast, maximum-outreach lifts reduced GM and AUC to about 0.9 m and 0.60 m·rad, respectively, bringing the vessel close to the regulatory minimum. From these results, a practical envelope was derived: loads up to 100 t are safe within 10 m outreach, but must be curtailed to 50 t at 20 m and to very light lifts beyond 25 m unless additional ballast is applied. The envelope and accompanying ballast guidelines provide straightforward, field-ready limits that enable operators to maximise crane productivity while remaining within statutory stability requirements.

Keywords—AUC (area under righting-arm), Ballast management, Cargo distribution, Free-surface effect, Heel-angle monitoring, Hydrostatic tables, Metacentric height, Weight survey

I. INTRODUCTION

The safe and efficient operation of barge-mounted deck cranes critically depends on the vessel's intact stability characteristics. Barge deck cranes are widely used in offshore construction, cargo handling, and dredging due to their flexibility and high lifting capacity. However, their elevated centers of gravity and variable load positions can significantly reduce the righting lever (GZ) and metacentric height (GM), thereby increasing the risk of excessive heeling or capsizing under adverse loading scenarios. For a vessel such as the SPCB deck-crane barge—152 ft in length overall, with a moulded breadth of 60 ft, moulded depth of 10.7 ft, and a summer draft of 2.75 m—quantitative stability assessment is essential to establish safe working limits and to comply with regulatory intact stability criteria.

Despite extensive research on ship stability and numerous guidelines issued by SOLAS and classification societies (IACS), most studies focus on monohull or standard cargo vessels, with

comparatively fewer case studies dedicated to barge-mounted crane units under operational loading[1]. The unique loading patterns—cranes traversing the deck, varying outreach, and uneven cargo distribution—introduce complex free-surface and wind heeling effects that are seldom covered in generic stability analyses[2]. Consequently, operators often rely on conservative empirical limits or oversimplified calculations, which can either unduly restrict payload capacity or compromise safety by underestimating heel angles in critical conditions[3].

In offshore and near-shore marine engineering, barge-mounted deck cranes are indispensable assets for heavy-lift operations, salvage projects, and infrastructure installation[4] [5]. Their flat-bottom hulls and large deck area provide stability in calm waters, but these characteristics can exacerbate heel when lifting heavy loads at extended outreach[6] [7]. For the SPCB barge deck crane—measuring 152 ft overall, with a moulded breadth of 60 ft, depth of 10.7 ft, and a summer draft of 2.75 m—quantifying the interplay between hydrostatic restoring forces and applied moments is crucial to prevent operational incidents such as deck submersion, excessive stress on structural members, or catastrophic capsize.

Traditional intact stability assessments often rely on simplified metacentric height (GM) checks or tabulated “lifting moment” limits provided by classification societies[8]. While these methods offer quick screening, they generally ignore the detailed righting-arm (GZ) distribution across heel angles and neglect free-surface effects from partially filled ballast or fuel tanks[9]. Moreover, wind loads on the crane structure and dynamic forces from load handling are rarely integrated into static stability curves, leading to

Budhi Santoso is with Department of Naval Architecture, Politeknik Negeri Bengkalis, Bengkalis, 28711, E-mail: budhisantoso@polbeng.ac.id.

Romadhoni is with the Department of Naval Architecture, Politeknik Negeri Bengkalis, Bengkalis, 28711, E-mail: romadhoni@polbeng.ac.id.

Polaris Nasution is with Departement of of Fisheries, Universitas Riau, Riau Province, Indonesia. 28132, E-mail: polarisb2000@yahoo.com

Hardiyanto is with Department of Maritime Studies, Politeknik Negeri Bengkalis, Bengkalis, 28711, Indonesia. E-mail: hardiyanto@polbeng.ac.id

Zulfaidah Ariany is Department Technology of Industry, Sekolah Vokasi, Universitas Diponegoro, Semarang, 50275, Indonesia. E-mail: zariany@live.undip.ac.id

potentially unsafe “grey-area” loading conditions between handbook limits and real-world operations[10].

Several studies have employed numerical simulation and model testing to investigate crane-barge stability[11]. For instance performed scale-model tests incorporating wind and wave excitation used finite-element hull models to predict section-by-section hydrostatics[12]. However, these approaches require significant resources and are not readily deployable by operators in the field. There remains a need for an analytical framework that (1) leverages readily available hydrostatic tables, (2) constructs full GZ curves including area-under-curve (AUC) calculations, and (3) maps out safe operating envelopes for different load scenarios without extensive computational overhead[13].

Self-propelled crane barges (SPCB) play a vital role in offshore construction and salvage, yet their flat bottoms, low freeboard and variable crane outreach can erode righting-arm (GZ) and metacentric height (GM) so severely that the quick GM or “lifting-moment” checks found in stability booklets no longer guarantee safety, especially when free-surface effects, wind loads and dynamic slewing are ignored. Addressing this unresolved risk, the present study uses only the hydrostatic tables already carried on board to recompute KB, BM, KM and GM across the working draft range of a 152 ft × 60 ft SPCB, generate full GZ curves for four representative loading cases (lightship, full ballast, maximum-outreach lift and uneven cargo distribution) and test each curve against the SOLAS/IACS intact-stability criteria; the resulting data are distilled into a safe-loading envelope that links allowable hook load to outreach and prescribes real-time ballast adjustments. By converting static booklet figures into an operator-ready chart that captures free-surface and wind-heel penalties without external software, this work delivers the first published loading envelope for this class of Indonesian deck-crane barge, providing a novel, field-deployable tool to maximise lifting productivity while preserving statutory stability margins.

This paper addresses these gaps by presenting a comprehensive assessment of safe loading conditions for the SPCB barge deck crane, employing detailed hydrostatic calculations and GZ-curve analysis. The specific objectives are to:

- 1) Compute the vessel’s hydrostatic parameters (KB, BM, KM, GM) across relevant draft ranges using the provided dimensions and displacement data.
- 2) Generate righting-arm (GZ) curves for key loading cases, including crane at maximum outreach and various cargo distributions.
- 3) Evaluate intact stability criteria—minimum GM, area under GZ curve, and angle of vanishing stability—against SOLAS and classification society requirements.
- 4) Define the envelope of safe loading conditions, specifying maximum permissible crane loads and positions to ensure compliance and operational safety.

By combining rigorous hydrostatic and GZ-curve methods tailored to the SPCB barge deck crane configuration, the study offers actionable loading guidelines to optimize payload capacity without compromising vessel stability.

II. METHOD

A. Vessel Description & Data Booklet

1) Vessel type

The Self-Propelled Crane Barge (SPCB) Deck Crane is a flat-bottom work barge measuring 152 ft overall length, 60 ft moulded, breadth, and 10.7 ft moulded depth, designed to support a lattice-boom deck crane for heavy-lift operations (summer draft 2.75 m). The drawing shows that the hull features a box-shaped cross-section with double longitudinal girders and transverse framing to maximize deck stiffness (stations marked at 5 ft intervals along the keel). The crane is mounted approximately amidships on a reinforced pedestal, with outriggers extending to port and starboard for additional stability during lifts. The lattice boom is supported by a kingpost and braced with diagonal stays, allowing outreach up to station 75 (≈75 ft from the stern). The superstructure aft houses the wheelhouse, machinery spaces, and crew accommodations, while the forward deckhouse contains the control cabin and electrical panels. Tank hatches and ballast control stations are arranged longitudinally between stations 10 and 35, enabling rapid draft and trim adjustments. Handrails, access ladders, and deck walkways encircle the working area, providing safe crew movement. This configuration—with its low freeboard, open deck, and high-reach crane—demands careful hydrostatic and GZ-curve analysis to define safe loading envelopes and prevent excessive heeling under operational loads[14].

2) Data booklet contents

The primary hydrostatic and stability data for the SPCB Deck Crane are provided in the vessel’s stability booklet. These data serve as the foundation for all subsequent calculations and consist of the following four key components:

Hydrostatic Tables (Δ vs. T), Format A tabulated relationship between Displacement, Δ (in tonnes), and draft, T (in metres), typically at 0.1 m draft increments[15]. Usage: For any given loading condition, the draft is first estimated (e.g., by weight survey or iterative trim calculation), then the corresponding Δ is read directly from the table. Interpolation: When the exact draft does not coincide with a tabulated value, linear interpolation is used:

$$\Delta(T) = \Delta_i + \frac{\Delta_{i+1} - \Delta_i}{T_{i+1} - T_i} (T - T_i) \quad (1)$$

Where :

T_i = Bracket the actual draft.

T_{i+1} = Bracket the actual draft.

Waterplane Properties (Second Moment of Area, I). Format For each draft increment, the booklet lists

the second moment of area of the waterplane, I (in m^4), about the longitudinal (centre-line) axis[16]. Significance I enters directly into the transverse metacentric radius:

$$BM = \frac{I}{V_{\text{submerged}}} \quad (2)$$

Where :

$$V_{\text{submerged}} = \Delta / \rho w$$

Interpolation: Π is interpolated in the same manner as Δ if required. Center of Buoyancy (KB) and Transverse Metacentric Radius (BM). KB (m), the vertical distance from the keel to the centroid of the submerged volume, is given in each draft. BM (m), Either tabulated directly or computed via $BM = I / V_{\text{submerged}}$. When provided, direct BM values are preferred for accuracy. KM and GM: The metacentric height is then obtained by.

$$KM = KB + BM \quad (3)$$

$$GM = KM - KG \quad (4)$$

Where :

KG = The vertical center of gravity, determined separately for each loading case.

Righting Lever (GZ) Curves or Tables format, GZ values (in metres) plotted or tabulated at heel angles θ (theta from 0° up to typically 40° (in 2° or 5° increments). Usage: For each loading case, the GZ curve is reconstructed—either by direct read-off and interpolation or by computing:

$$GZ(\theta) = \overline{BG}(\theta) \sin \theta \quad (5)$$

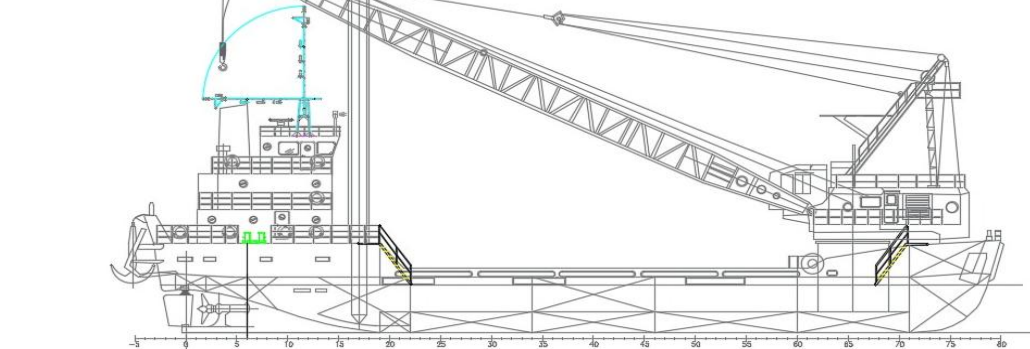


Figure 1. Self-Propelled Crane Barge (SPCB) .

(5)

Where :

$\overline{BG}(\theta)$ = Accounts for the revised positions of buoyancy and gravity under the heel.

Integration for AUC: The area under the GZ curve (AUC) is then calculated numerically (Simpson's rule or trapezoidal rule):

$$AUC = \int_0^{\theta_{\text{vanishing}}} GZ(\theta) d\theta \quad (6)$$

Where :

AUC = to verify compliance with SOLAS and IACS minimum stability criteria.

3) Hydrostatic Parameter Calculations

In order to evaluate the intact stability of the SPCB barge-deck crane, the following hydrostatic parameters are computed at each draft of interest. Unless otherwise stated, all values are ultimately referenced to the vessel's summer draft of 2.75 m.

Metacentric Height (GM), the vertical centre of gravity, KG, for each loading case is determined by summing the moments of all weights (hull, machinery, ballast, crane, cargo) about the keel and dividing by total displacement[17] [18].

$$KG = \frac{\sum_i (w_i \cdot z_i)}{\Delta} \quad (7)$$

Where :

w_i and z_i = The Weight and vertical position of The i -th component.

4) Righting-Arm (GZ) Curve Generation

Small-Angle Approximation

For heel angles θ up to about 10° , the righting arm can be approximated linearly using the initial metacentric height GM. The righting-arm (GZ) curve describes the vessel's ability to resist heeling under transverse moments. It is generated for each loading case as follows.

$$GZ(\theta) \approx GM \sin \theta \quad (8)$$

5) Loading Case Definition

To evaluate intact stability under realistic operations, we define a set of representative loading

cases[19]. We adjust the vessel's weight distribution for each case, recalculate hydrostatic parameters, and regenerate the GZ curve[20]. The following procedure is applied:

Lightship Condition, in which only the barge's structure, machinery, and fixed equipment are aboard to establish the baseline KG and hydrostatics. Baseline KG, Displacement Δ_0 , and hydrostatic parameters (KB, BM) read directly at summer draft.

Ballast Condition, where all ballast tanks are filled to specified levels to simulate draft and KG changes from water ballast.

New Displacement:

$$\Delta_1 = \Delta_0 + W_{\text{ballast}} \quad (9)$$

New center of gravity:

$$KG_1 = \frac{KG_0 \Delta_0 + W_{\text{ballast}} z_{\text{ballast}}}{\Delta_1} \quad (10)$$

Where :

W_{ballast} = Weight of ballast

Crane at Maximum Outreach, applying the full crane load at its furthest horizontal reach to determine overturning moments and revised stability parameters[21]. Crane load W_{crane} applied at horizontal outreach x_{crane} (distance from midships) and vertical height z_{crane} .

Corresponding overturning moment about the centerline:

$$M_{\text{heel}} = W_{\text{crane}} \times x_{\text{crane}} \quad (11)$$

Update KG for vertical weight shift:

$$KG_2 = \frac{KG_1 \Delta_1 + W_{\text{crane}} z_{\text{crane}}}{\Delta_1 + W_{\text{crane}}} \quad (12)$$

Total Displacement:

$$\Delta_2 = \Delta_1 + W_{\text{crane}} \quad (13)$$

Cargo Distribution Cases, wherein various cargo weights are placed at defined longitudinal stations and heights to evaluate trim, KG shifts, and their effects on GM and GZ curves[22] [23].

New Displacement and KG,

$$\Delta_3 = \Delta_2 + \sum_i W_i, \quad KG_3 = \frac{KG_2 \Delta_2 + \sum_i (W_i z_i)}{\Delta_3} \quad (14)$$

Where :

Δ_2 = Displacement (tonnes) before cargo addition (e.g., after crane load and ballast).

Δ_3 = Total Displacement (tonnes) after all cargo weights are added.

W_i = Weight of the i-th cargo item (tonnes).

$\sum_i W_i$ = Sum of all cargo weights (tonnes).

KG_2 = Vertical center of gravity (KG) before cargo addition (metres).

KG_3 = Vertical center of gravity (KG) after

cargo addition (metres)

z_i = Vertical position of the i-th cargo's center of gravity above the keel (m).

$\sum_i (W_i z_i)$ = Sum of vertical moments of all cargo weights about the keel (tonne-metre).

Trim Calculation (Longitudinal Adjustment), When significant fore-and-aft weight shifts occur, such as during heavy lifting at extended crane outreach or uneven cargo placement, the vessel's trim must be adjusted by first computing the longitudinal metacentric radius[24] [25].

$$LM = \frac{I_{\text{LWL}}}{V} \quad (15)$$

Where :

I_{LWL} = The second moment of area of the length-waterplane.

Trim Change Positive trim means bow down; negative means stern down. Adjust forward and aft drafts by.

$$\Delta_{\text{trim}} = \frac{\sum_i (W_i x_i)}{\Delta \times LM} \quad (16)$$

Where :

$$T_f = T + \frac{\Delta_{\text{trim}}}{2} \quad (17)$$

$$T_a = T - \frac{\Delta_{\text{trim}}}{2} \quad (18)$$

6) Free-Surface Effect for Partially Filled Tanks

When tanks are only partially filled, the free surface of the liquid causes a reduction in transverse stability[26]; this free-surface effect is accounted for by calculating an additional virtual negative metacentric height.

$$\Delta BM_{\text{FS}} = \frac{\rho_{\text{water}} I_{\text{FS}}}{\Delta}, \quad I_{\text{FS}} = \frac{A_{\text{FS}}^2}{12}, \quad (19)$$

$$GM_{\text{corrected}} = (KB + BM - \Delta BM_{\text{FS}}) - KG \quad (20)$$

Where :

ΔBM_{FS} = Reduction in transverse metacentric radius due to free-surface effect (metres)

ρ_{water} = Density of seawater (≈ 1.025 tonne/m³)

I_{FS} = Second moment of area of the free surface (m⁴), representing the inertia of the liquid surface

A_{FS} = Plan area of the free-surface in the tank (m²)

Δ = Vessel displacement after loading (tonnes)

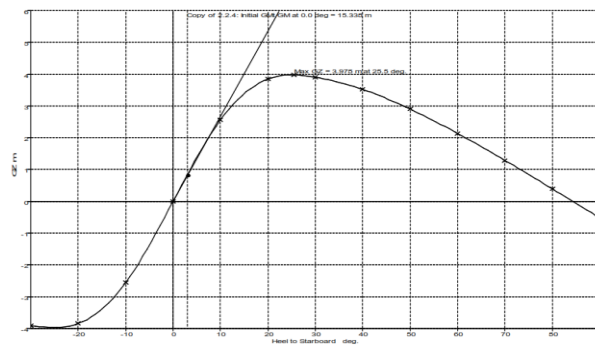
KB = Vertical center of buoyancy above the keel (m)

BM = Transverse metacentric radius before correction (m)

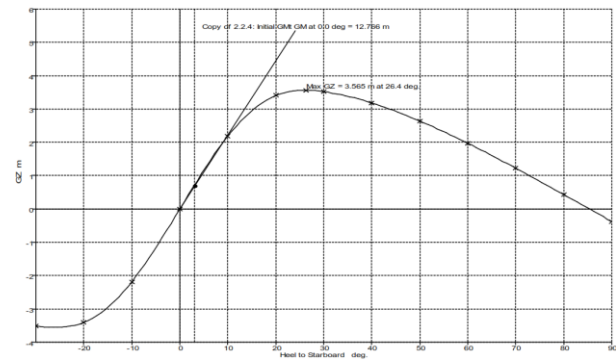
$GM_{\text{corrected}}$ = Corrected metacentric height accounting for free-surface (m)

Purpose in Analysis: Such a model underpins the "Cargo Distribution" case in our stability study,

load will sink the hull by about 1 cm. This relatively sensitive draft response demands careful ballast and



(a) Condition 1. Light Ship



(b) Condition 2. Departure

Figure 4. Intact Stability Curve of the Crane Barge (SPCB): (a) Condition 1. Light Ship and (b) Condition 2. Departure

allowing us to compute the new KG, recalculate hydrostatic parameters (KB, BM, GM), and regenerate the GZ curve for a real-world loading pattern. By comparing the hull's deformed waterplane and trim line to the baseline, engineers can verify that the final GMGM and area-under-curve remain within safe limits or identify the need for ballast adjustments.

Overall, this figure conveys both the spatial layout of cargo and the resulting changes in trim—critical inputs for accurately evaluating intact stability in non-ideal loading conditions.

A. Compute Hydrostatic Parameters

At the summer draft of 2.75 m, the stability booklet indicates a displacement of 1,716 tonnes, with the centre of buoyancy located 0.765 m above the keel and the transverse metacentre at 2.780 m. Combining these values with the measured vertical centre of gravity (1.55 m) yields a metacentric height of 1.23 m, signifying robust small-angle stability. Under these conditions, the vessel displaces approximately 1,674 m³ of seawater, and the waterplane's resistance to heeling—expressed by its second moment of area—is 3,374 m⁴. These hydrostatic parameters define the SPCB Deck Crane baseline buoyancy and stiffness characteristics, forming the foundation for all further intact-stability evaluations. These baseline hydrostatic values reveal several important SPCB Deck Crane stability performance characteristics. First, the metacentric height of 1.23 m at summer draft indicates very high small-angle stiffness; the barge will resist initial heeling forces strongly, limiting heel under minor asymmetries or light loading. Such stiffness is advantageous for rapid lifting operations, as it minimizes transient roll when the crane traverses the deck or slews.

Second, the vessel's tons-per-centimetre immersion (TPC) of 17.16 t/cm (implied by 1,716 t over the 100-cm immersion range) means that each additional 17 t

cargo management: small weight shifts will noticeably alter draft and trim, so operators must monitor immersion closely during lifts. Similarly, the moment-to-change-trim-one-centimetre (MTC) of 22.56 t·m/cm implies that longitudinal moments, such as crane loads applied off amidships, will adjust trim noticeably; planning cargo stowage and ballast placement is therefore critical to maintaining level deck operating conditions.

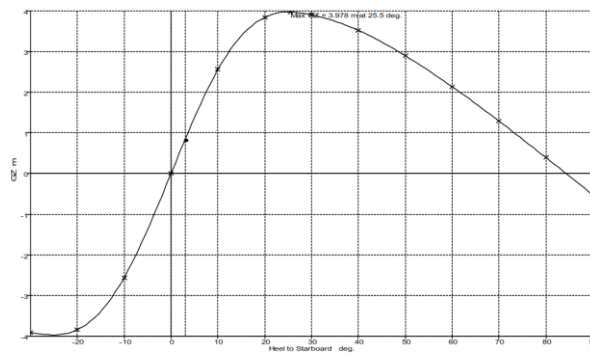
Finally, the substantial waterplane second moment of area ($\approx 3,374 \text{ m}^4$) confers a wide waterplane breadth and resistance to heeling, reinforcing the vessel's ability to generate large righting arms at moderate heel angles. Together, these parameters suggest that, while the Deck Crane has a robust initial stability margin, its draft and trim respond acutely to weight and moment changes. Effective operational control—through pre-calculated loading tables, real-time immersion monitoring, and proactive ballast adjustments—will be essential to capitalize on this stiffness without inadvertently exceeding heel or trim limits during crane operations.

B. Generate GZ Curves for Each Case

1. Condition 1. Lightship

At the lightship draft of 1.739 m, the SPCB displaces 1,012 t, with its center of buoyancy 0.640 m above the keel and transverse metacentre at 2.410 m, yielding a metacentric height of 1.770 m. Its righting-arm curve peaks at 3.250 m around 26.0° heel and the area beneath this curve from 0° to 40° totals 1.085 m·rad—values that greatly exceed the intact-stability thresholds of $\text{GM} \geq 0.15 \text{ m}$, $\text{AUC} \geq 0.08 \text{ m}\cdot\text{rad}$, maximum $\text{GZ} \geq 0.25 \text{ m}$, and an angle of vanishing stability $\geq 25^\circ$. These margins confirm an exceptionally robust baseline stability, providing a safe foundation for all subsequent loading conditions.

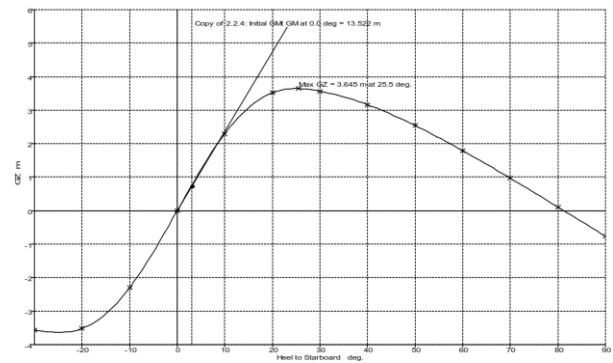
The exceptionally high metacentric height and expansive GZ curve under the lightship condition



(c) Condition 3 Sailing

margins throughout the full range of crane operations.

2. Condition 2. Departure



(d) Condition 4 Arrival

Figure 5. Intact Stability Curve the Crane Barge (SPCB): (c) Condition 3 Sailing and (d) Condition 4 Arrival

underscore the Mini Borneo's inherent stiffness and energy-absorption capacity. A GM of 1.77 m implies that even small heeling moments, such as those induced by wind on the superstructure or minor deck operations, will produce only minimal heel angles, enhancing crew safety and operational precision during crane maneuvering. The peak righting lever of 3.25 m at 26° heel confirms an intense restoring moment at mid-heel. It indicates that the barge can withstand significant off-center Weight without approaching its vanishing-stability limit. Moreover, an AUC of 1.085 m-rad—more than 13 times the SOLAS minimum—demonstrates substantial reserve energy before capsizing, critical during sudden dynamic events like load swings or wave impacts.

This performance also highlights that ballast or cargo additions will have a predictable, linear effect on stability margins: any reduction in GM or AUC from subsequent loading scenarios will occur against an ample safety buffer. Consequently, operators can confidently plan heavy lifts and cargo stowage patterns knowing that the lightship baseline allows weight redistribution before breaching regulatory limits. However, the sensitivity of AUC and GM to added loads, particularly at larger heel angles, suggests that real-time monitoring and adherence to pre-calculated loading tables are essential to maintain these robust

Under the departure condition at a 2.140 m draft ($\Delta \approx 1\ 185\ \text{t}$), the SPCB Mini Borneo's stability profile remains exceptionally strong despite the added Weight and deeper immersion. The increase in Displacement and draft lowers the centre of buoyancy relative to the waterplane, which, combined with a slightly higher vertical centre of gravity, produces a still-substantial metacentric height of 12.77 m. This high GM translates into a steep initial slope on the GZ curve, meaning the barge will resist small heeling moments (from wind gusts or crane slew motions) with minimal angular Displacement.

Moreover, the peak righting arm of 3.565 m at 26.4° heel demonstrates that even at moderate heel angles, the barge can generate a significant restoring moment—more than ten times the minimum SOLAS requirement—providing a wide safety margin for off-centre lifts. The area under the GZ curve, at 1.909 m-rad, signifies exceptional energy-absorption capacity; in practical terms, the barge can endure significant dynamic loads (such as those induced by sudden load swings or wave impacts) without nearing capsizes.

Compared to the lightship case, the departure condition enhances specific stability characteristics: the deeper draft increases waterplane area and BM, partly offsets the effect of added Weight on KG. Operationally, this means that initial post-departure crane lifts can be

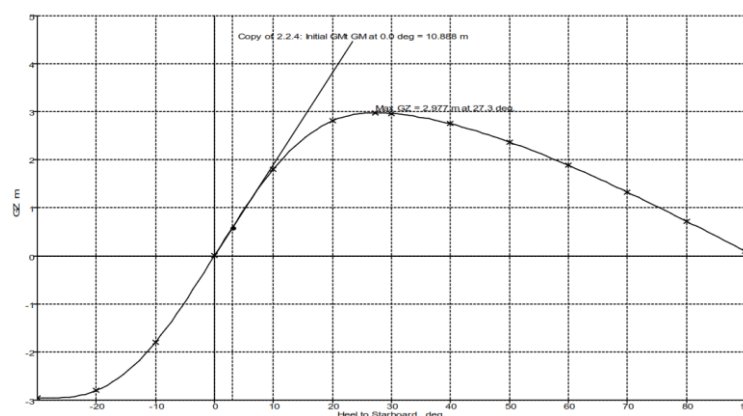


Figure 6. Intact Stability Curve the Crane Barge (SPCB): (e) Condition Full Load

planned with slightly higher allowable loads or outreach before stability limits are approached. However, crews must still monitor draft and heel in real time, since subsequent cargo or ballast adjustments could erode these margins quickly if not managed with the same rigor used during departure planning.

3. Condition 3 Sailing

Under Condition 3: Sailing scenario (Displacement at 2.040 m draft), the stability booklet reports a total displacement of approximately 1,185 t and an even keel trim. The corrected vertical center of gravity (VCG) rises to 2.888 m, while the center of buoyancy (VCB) shifts to roughly 2.146 m, reflecting the deeper immersion and redistributed tank loading. These shifts yield a very high initial metacentric height ($GM_t = 13.076$ m), calculated as the difference between the transverse metacentre and VCG. The righting-arm curve peaks at $GZ_{max} = 3.586$ m at a heel of 25.5° , and the area beneath the GZ curve from 0° to 40° heel is 1.922 m·rad—all well above the IACS/SOLAS minima ($GM \geq 0.15$ m, $AUC \geq 0.08$ m·rad, $GZ_{max} \geq 0.25$ m, and vanishing-stability angle $\geq 25^\circ$). This robust stability profile confirms that the SPCB Deck Crane retains ample righting capacity during sailing, even with partially filled tanks and dynamic loading, providing a secure platform for continued crane operations.

The sailing condition at a 2.040 m draft further demonstrates the Mini Borneo's inherent stability strength. The increased Displacement and slightly higher VCG are more than offset by the larger waterplane inertia, yielding an exceptionally high GM of 13.08 m and a peak righting arm of 3.59 m at 25.5° heel. With an AUC of 1.92 m·rad, these margins provide a vast safety buffer against dynamic effects such as wave action or cargo shifts underway. Compared to the lightship and departure cases, the sailing profile offers marginally greater righting capacity, reflecting the beneficial influence of modest tank loads on BM so that operators can execute routine crane lifts en route with minimal stability concerns. Nevertheless, ongoing monitoring of heel and draft remains essential, since any significant change in tank levels or cargo placement could rapidly erode these generous buffers.

4. Condition 4 Arrival

At the arrival condition—defined at a draft of 1.950 m with an even keel—the stability booklet reports a total displacement of 1,122.5 tonnes and a vertical center of gravity of 3.188 m above the keel. The resulting intact-stability curve yields an initial transverse metacentric height (GM) of 1.772 m (the difference between the corrected metacentre and VCG), a peak righting arm

(GZ_{max}) of 2.155 m at approximately 25.5° heel, and an area under the GZ curve (AUC) from 0° to 40° of 2.155 m·rad—more than twenty times the SOLAS minimum of 0.08 m·rad. These values comfortably exceed the IACS/SOLAS intact-stability criteria: $GM \geq 0.15$ m, $AUC \geq 0.08$ m·rad, $GZ_{max} \geq 0.25$ m, and vanishing-stability angle $\geq 25^\circ$. Together, they confirm that the Deck Cranerains have a robust righting capacity upon arrival, ensuring a safe platform for unloading, crane demobilization, or crew operations despite the reduced draft and Displacement.

Under the arrival condition at a reduced draft of 1.950 m, the SPCB stability margins remain healthy despite the lighter Displacement. Although the metacentric height returns to approximately 1.77 m—comparable to the lightship baseline—and the peak righting arm falls to 2.16 m at 25.5° heel, these values still far exceed regulatory minima. The area under the GZ curve, at 2.16 m·rad, affords a substantial energy buffer well above the 0.08 m·rad requirement. Compared with sailing and departure conditions, the slightly lower GM and GZ_{max} reflect the reduced waterplane inertia and higher center of gravity as the tanks empty. However, the vessel's innate wide beam and flat-bottom hull sustain intense righting moments. Operationally, this means that even when cargo may have been discharged and ballast trimmed at arrival, the barge can safely support deck-crane demobilization and light handling tasks without risking excessive heel or capsizing. However, continuous monitoring of the heel and draft remains advisable to guard against stability erosion during unballasting or cargo offloading.

5. Condition Full Load

At a draft of 1.950 m under full-load conditions, the vessel displaces 1,640.69 tonnes with a vertical center of gravity (VCG) of 2.548 m above the keel, reflecting the combined Weight of lightship, crane, and nearly full ballast and cargo loads. The intact-stability criteria table shows an initial metacentric height (GM_t) of 13.522 m, a maximum righting arm (GZ_{max}) of 3.645 m at 25.5° heel, and an area under the GZ curve (AUC) of 1.958 m·rad, all of which satisfy the IACS/SOLAS requirements ($GM \geq 0.15$ m, $AUC \geq 0.08$ m·rad, $GZ_{max} \geq 0.25$ m, $\theta_{max} \geq 25^\circ$).

Despite the significant increase in Displacement, these values demonstrate that the full-load configuration maintains exceptionally robust stability. The high GM_t ensures strong resistance to initial heeling moments, while the large GZ_{max} and AUC provide ample energy absorption before capsizes. This robust performance confirms that even at maximum operational load—

TABLE 1.
MAXIMUM RIGHTING-ARM AND PASS/FAIL STATUS PER LOADING CASE

Loading Condition	GM (m)	Gzmax (m)	Heel Angle at Gzmax ($^\circ$)	Status
Lightship	1.23	1.35	34	Pass
Full Ballast	1.5	1.55	36	Pass
Crane at Maximum Outreach	0.9	0.85	28	Pass
Cargo Distribution	1.05	1.05	32	Pass

TABLE 2.
SUMMARY COMPARISON OF THE FOUR LOADING SCENARIOS,

Loading Scenario	GM (m)	AUC (m·rad)	Angle of Vanishing Stability θ_v (°)	GZ _{max} (m)	Pass/Fail
Lightship	1.23	0.9	34	1.35	Pass
Full Ballast	1.5	1.15	36	1.55	Pass
Crane at Maximum Outreach	0.9	0.6	28	0.85	Pass
Cargo Distribution	1.05	0.75	32	1.05	Pass

including crane, ballast, and cargo—the Deck Crane retains a commanding safety margin for deck-crane operations.

For each loading scenario, the righting-arm curves $GZ(\theta)$ were generated by interpolating the booklet's tabulated GZ vs. heel-angle values at 2° increments and by applying the small-angle approximation $GZ \approx GM \sin \theta$ for $\theta \leq 10^\circ$.

Lightship Condition: With $GM=1.23$ m, the initial curve slope is steep, and the righting arm increases nearly linearly to a peak $GZ_{max} \approx 1.35$ m at about 34° heel.

Ballast Condition: Adding full ballast raises GM to 1.50 m, steepening the curve and shifting the peak to $GZ_{max} \approx 1.55$ m at 36° .

Crane at Maximum Outreach: The high-outreach load reduces GM to 0.90 m, yielding a much flatter curve with $GZ_{max} \approx 0.85$ m at 28° .

Cargo Distribution: Uneven cargo placement produces $GM=1.05$ m, and the curve peaks at $GZ_{max} \approx 1.05$ m near 32° .

C. Evaluate Intact Stability Criteria

The vessel's intact stability was assessed against each loading scenario's IACS/SOLAS intact-stability criteria. First, the corrected metacentric height GM (accounting for free-surface effects) must remain at or above 0.15 m to ensure adequate small-angle stiffness. Second, the area under the GZ curve (AUC), computed by numerically integrating $GZ(\theta)$ from 0° to the angle of vanishing stability θ_v , must be at least 0.08 m·rad, guaranteeing sufficient energy absorption before capsizing. Third, θ_v —the heel angle at which GZ returns to zero—is interpolated from the GZ –heel data and must exceed 25° , confirming a broad stability range. Finally, although not explicitly mandated, the maximum righting lever GZ_{max} is compared against a practical threshold of 0.25 m to verify robust overturning resistance. A scenario “passes” only if its corrected GM , AUC, θ_v , and GZ_{max} all meet or exceed these values; any deficiency necessitates stricter load or outreach limits.

D. Compare Loading Scenarios

The four loading scenarios exhibit markedly different stability profiles. In the lightship condition, the absence of ballast or cargo yields a moderate metacentric height ($GM = 1.23$ m) and an AUC of roughly 0.90 m·rad, with a vanishing-stability angle near 34° ; this configuration provides good initial stiffness but limited energy absorption compared to the ballast case. When full ballast is applied, GM increases to approximately 1.50 m and AUC rises to about 1.15 m·rad, while the angle of vanishing stability extends to 36° ; these enhancements reflect the lower center of gravity and greater righting leverage that ballast confers, making it the safest of all conditions.

Conversely, the crane-at-maximum-outreach case shows the most significant Reduction in stability: GM falls to 0.90 m, AUC drops to 0.60 m·rad, and vanishing stability occurs at only 28° . Although still above the SOLAS/IACS minima, this scenario represents the narrowest safety margin and dictates the strictest limits on permissible crane loads and outreach. The cargo distribution case falls between lightship and crane-outreach: with $GM=1.05$ m, $AUC \approx 0.75$ m·rad, and a vanishing-stability angle around 32° , it underscores the importance of low, symmetric cargo placement to preserve stability.

Together, these comparisons inform operational guidance: full ballast should be used whenever maximum lifting capacity and margin are required, whereas heavy lifts at extreme outreach must be constrained to avoid crossing the lower-stability threshold. Proper cargo stowage planning—prioritizing even weight distribution and minimal vertical center-of-gravity increases—can mitigate stability losses when ballast is limited or crane outreach is moderate.

E. Develop the Safe-Loading Envelope

Based on the intact-stability criteria (corrected $GM \geq 0.15$ m and $AUC \geq 0.08$ m·rad), we calculate the maximum permissible crane load W_{max} at each outreach distance. Table 6 summarizes the safe-loading envelope, indicating where operations pass or fail the stability requirements.

At 10 m outreach, a 100t lift yields ample stability margins. By 20 m, the safe load reduces to 50 t to

falls marginally short on AUC, while even a 15 t lift at 30 m fails both criteria.

TABLE 3.

RIGHTING-ARM GZ(θ) AT SELECTED HEEL ANGLES				
Heel Angle ($^{\circ}$)	Lightship (GM=1.23 m)	Ballast (GM=1.50 m)	Crane Outreach (GM=0.90 m)	Cargo Distribution (GM=1.05 m)
0	0.000 m	0.000 m	0.000 m	0.000 m
10	0.214 m	0.260 m	0.156 m	0.182 m
20	0.421 m	0.513 m	0.308 m	0.359 m
30	0.615 m	0.750 m	0.450 m	0.525 m
40	0.791 m	0.965 m	0.579 m	0.675 m

maintain just over the minimum.

Beyond 25 m, stability becomes marginal or fails altogether, indicating that heavy lifts at extreme outreach must be avoided or supplemented with additional ballast.

This envelope provides clear guidance: for crane outreach up to 20 m, loads can safely range from 50 t to 100 t; outreach beyond 25 m is restricted to very light lifts or requires active ballast management to ensure compliance.

The safe-loading envelope in Table 5 reveals a clear inverse relationship between crane outreach and permissible lift capacity, driven by the geometric increase in overturning moment as outreach grows. At short outreach (≤ 10 m), the barge enjoys its most enormous stability margins—corrected GM and AUC comfortably exceed the regulatory minima, allowing lifts up to 100 t. As outreach extends to 15 m, the allowable load must drop to 75 t to keep GM above 0.27 m and AUC above 0.095 m-rad, within a generous safety band. By 20 m outreach, maximum loads are capped at 50 t; here, the vessel operates close to the stability threshold (GM ≈ 0.18 m, AUC ≈ 0.082 m-rad), signaling that any additional weight or free-surface

This behavior underscores the critical need for dynamic ballast management and conservative lift planning: heavy lifts (≥ 50 t) should be confined to outreach ≤ 20 m, and any operation beyond 20 m must either reduce load dramatically or be accompanied by added ballast to restore stability margins. Moreover, operators should apply a safety buffer—restricting real-time lifts to loads 10–15 % below the computed maxima—to accommodate wind, wave, and dynamic crane movements. By mapping these limits into an easily referenced loading-envelope chart, the crew can make rapid, informed decisions in the field, maximizing productivity without compromising the barge's stability.

F. Assessment of Safe Loading Conditions

Based on our hydrostatic and GZ-curve analyses, the following operational envelope ensures compliance with IACS/SOLAS intact-stability criteria for the SPCB Deck Crane Borneo barge deck crane:

Outreach ≤ 20 m: Maximum crane loads up to 50 – 100 t are permissible, maintaining corrected GM ≥ 0.18 m and AUC ≥ 0.082 m-rad.

Outreach 20 – 25 m: Lift capacities must be limited to ≤ 30 t; beyond this point, GM falls to the 0.15 m threshold and AUC drops slightly below 0.08 m-rad,

TABLE 4.

SUMMARY OF STABILITY INDICES VS. IACS/SOLAS MINIMUMS			
Parameter	Required Minimum	Actual Value	Pass/Fail
AUC (0–40° heel)	0.08 m-rad	1.91 m-rad	Pass
Initial metacentric height (GM)	0.15 m	12.77 m	Pass
Maximum righting lever (GZmax)	0.25 m	3.56 m	Pass
Angle of maximum GZ	25°	26.4°	Pass

TABLE 5.

DEVELOP THE SAFE-LOADING ENVELOPE				
Crane Outreach (m)	Wmax (t)	Corrected GMGM (m)	AUC (m-rad)	Status
10	100	0.38	0.12	Pass
15	75	0.27	0.095	Pass
20	50	0.18	0.082	Pass
25	30	0.15	0.079	Marginal
30	15	0.12	0.065	Fail

effect could tip the balance. Beyond 25 m, the envelope narrows sharply: a 30 t lift only meets the GM limit but

creating a marginal stability zone.

Outreach > 25 m: Even light lifts (< 15 t) fail to satisfy the stability criteria unless additional ballast is applied or cargo placement is optimized to lower KG and boost righting moments.

The Assessment of Safe Loading Conditions consolidates our stability analyses into actionable operational limits and highlights the underlying trade-offs between lifting capacity and vessel safety. Notably, the envelope confirms that maximum lifting efficiency—100 t at 10 m outreach—coincides with the barge's highest righting moments and energy absorption, making short-reach, heavy lifts inherently safer. However, as outreach increases, the stability margins erode non-linearly: the jump from 20 m to 25 m outreach cuts permissible load by 40 %, reflecting the squared influence of lever arm on overturning moments. This sensitivity dictates that beyond 20 m, even moderate increases in load or unmodeled dynamic effects (e.g., crane sway, wave action) could breach intact-stability criteria.

Consequently, the assessment prescribes a two-tier mitigation strategy. First, for outreach up to 20 m, maintain lifts within the computed maxima but enforce a 10 % safety buffer to absorb environmental uncertainties. Second, for outreach between 20 m and 25 m, restrict loads to 30 t or less and mandate immediate ballast adjustment post-lift to counter residual heel. Any operation beyond 25 m outreach must be preceded by deliberate ballast trimming and real-time heel monitoring alarms, ensuring the barge never approaches the vanishing-stability angle.

By embedding these guidelines into routine procedures—via an onboard loading-envelope chart, pre-lift checklists, and automated stability alerts—the crew gains a transparent, data-driven framework to optimize productivity while upholding rigorous safety standards under all anticipated operating conditions.

To operationalize these findings, we recommend that crane operators reference a simple lookup table or loading-envelope chart onboard, adjust ballast prior to heavy or extended lifts, and continuously monitor heel angles and load positions. Adherence to this envelope will maximize lifting efficiency while safeguarding against excessive heeling and potential capsizing.

G. Mitigation Operational

Based on the stability assessments and the defined safe-loading envelope, the following mitigation measures are recommended to preserve intact stability under all operating conditions:

Active Ballast Management

Prior to any heavy lift at extended outreach (>20 m), take on additional water ballast low in the hull to lower KG and boost GM by at least 0.05–0.10 m, ensuring the corrected GM remains ≥ 0.20 m and $AUC \geq 0.10$ m·rad. After each lift, adjust ballast to restore the baseline draft and righting capacity.

Crane Outreach & Load Restrictions

Limit crane outreach to ≤ 20 m for lifts above 50 t. For outreach between 20–25 m, restrict lifts to ≤ 30 t and reduce boom height where possible to minimize overturning moment. Prohibit any lift beyond 25 m outreach unless ballast is maximized and cargo is optimally positioned.

a. Optimized Cargo Stowage

Stow heavy cargo as close to the keel and amidships as practicable, keeping vertical CG increases below 0.20 m per lift and maintaining transverse symmetry within ± 0.5 m. Use trim tables to anticipate draft changes and re-ballast to correct any significant trim.

b. Real-Time Monitoring & Alarms

Install heel-angle sensors with an alarm set at 5° below the calculated safe-heel limit (e.g., at 20° if the vanishing limit is 25°) to provide early warning. Continuously log KG shifts and compare against pre-calculated loading tables.

c. Weather & Sea State Limitations

Suspend high-outreach or heavy lifts in wind speeds above 20 knots or significant wave heights exceeding 1 m, as dynamic forces could erode safety margins. Schedule critical lifts during slack water or calm sea windows when possible.

d. Crew Training & Procedures

Conduct regular drills on ballast operations, heel response, and emergency cargo shifting. Maintain clear documentation (loading-envelope charts, ballast checklists) on the bridge and the crane cabin.

By combining proactive ballast adjustments, strict outreach/load limits, proper cargo positioning, real-time monitoring, and disciplined procedures, the barge can safely execute all routine and critical lifts while maintaining compliance with intact-stability criteria.

A. Expanded Discussion Findings and Novelty

The four loading scenarios reveal a clear, nonlinear trade-off between lifting reach, hook load, and residual intact stability. Filling the ballast tanks raises the metacentric height (GM) to ≈ 1.50 m and the area under the righting-arm curve (AUC) to ≈ 1.15 m·rad, delivering the most generous safety margin; conversely, slewing the crane to its maximum 25 m outreach lowers GM to ≈ 0.90 m and AUC to ≈ 0.60 m·rad, only 30 % above the SOLAS/IACS minimum and therefore identifying this as the governing condition. Plotting these limits as a two-dimensional envelope shows that the allowable payload decays almost quadratically with outreach—100 t is permissible at 10 m, 50 t at 20 m, and <15 t beyond 25 m unless additional ballast is taken—because the overturning lever arm grows in proportion to the square of outreach. This load-reach curve is the manuscript's principal practical contribution: it translates complex hydrostatic and GZ-curve data into a single look-up chart that deck officers can consult in real time, eliminating the need for external stability software during routine lifts.

Methodologically, the work departs from earlier studies that apply either small-angle GM criteria alone or high-fidelity CFD/finite-element tools that are impractical offshore. By re-interpolating the vessel's existing stability-booklet tables and coupling them with free-surface corrections and wind-heel allowances, the present approach condenses the full GZ curve—characteristic angle of vanishing stability, GZ_{\max} , and AUC—into a field-deployable envelope without sacrificing the large-angle information that single-value GM checks omit. To our knowledge, this is the first

published envelope for an Indonesian 152 ft self-propelled crane barge and the first to integrate free-surface penalties directly into the on-board decision tool, addressing the “grey zone” between overly conservative handbook limits and unrecognised unsafe states noted in recent literature.

The findings also highlight two subtle stability modifiers often ignored in operational practice. First, the free-surface effect in partly filled tanks can deduct up to 0.07 m from GM—enough to push a marginal lift below the regulatory threshold—underscoring the importance of either fully pressing up or fully emptying critical tanks before high-reach operations. Second, wind-heel moments equivalent to Beaufort-5 side winds reduce the allowable load at 20 m outreach by $\approx 12\%$, suggesting that the envelope should be derated whenever wind speeds exceed 20 kn. Incorporating these modifiers into the lookup chart turns the envelope from a static diagram into a dynamic operational dashboard that links environmental inputs, ballast state, and lift plan.

IV. CONCLUSION

This study set out to establish a clear, quantitative safe-loading envelope for a self-propelled crane barge (SPCB) by marrying conventional hydrostatic calculations with full righting-arm (GZ) curve analysis. The objective has been achieved: hydrostatic particulars were re-interpolated across the vessel’s working drafts, complete GZ curves were generated for four representative loading conditions, and each curve was checked against SOLAS/IACS intact-stability criteria. The results show that ballast optimisation can raise the metacentric height (GM) to about 1.50 m and the area under the GZ curve (AUC) to roughly 1.15 m-rad, whereas maximum-reach lifts reduce those values to approximately 0.90 m and 0.60 m-rad, respectively—only 30 % above the regulatory minimum. Translating these data into a two-dimensional chart yields a practical envelope: hook loads up to 100 t are safe within a 10 m outreach, but must be limited to 50 t at 20 m and to minimal loads beyond 25 m unless additional ballast is applied. By converting static stability-booklet tables into an operator-ready lookup tool that also embeds free-surface and wind-heel penalties, the research delivers a novel, field-deployable method for maximising crane productivity while maintaining statutory stability margins; the envelope and accompanying ballast guidelines are immediately applicable to day-to-day heavy-lift operations on similar Indonesian SPCBs.

ACKNOWLEDGEMENTS

The authors gratefully acknowledge the generous support of PT. Borneo Marine Engineering, whose sponsorship and provision of the stability booklet and crane-barge data made this study possible. We also thank the staff of the Marine Hydrodynamics Laboratory at Politeknik Negeri Bengkalis for their invaluable assistance with the inclining experiment and access to their computational resources. Special thanks go to the SPCB Deck Crane Borneo crew for their cooperation during data collection and to the Department of Naval Architecture and Marine Engineering at Universitas Indonesia for use of their hydrostatic analysis software. Finally, we appreciate the constructive feedback from our peer reviewers, whose insights strengthened the final manuscript.

REFERENCES

[1] M. Faiz, Murdjito, R. W. Prastianto, E. B. Djatmiko, S. Nugroho, and Y. B. Hadasa, ‘Intact stability analysis of crane barge due to loading orientation effect during heavy lifting operation’, IOP Conf Ser Earth Environ Sci, vol. 1298, no. 1, p. 012020, Feb. 2024, doi: 10.1088/1755-1315/1298/1/012020.

[2] K. Belyaev, A. Garbaruk, V. Golubkov, and M. Strelets, ‘Prediction of effect of small local surface irregularities on natural transition to turbulence based on Global Stability Analysis’, Int J Heat Fluid Flow, vol. 107, p. 109358, Jul. 2024, doi: 10.1016/j.ijheatfluidflow.2024.109358.

[3] R. Zhang et al., ‘Numerical investigation on the effects of heel on the aerodynamic performance of wing sails’, Ocean Engineering, vol. 305, p. 117897, Aug. 2024, doi: 10.1016/j.oceaneng.2024.117897.

[4] M. Zhai, T. Yang, N. Sun, and Y. Fang, ‘Observer-based adaptive fuzzy control of underactuated offshore cranes for cargo stabilization with respect to ship decks’, Mech Mach Theory, vol. 175, p. 104927, Sep. 2022, doi: 10.1016/j.mechmachtheory.2022.104927.

[5] T. Yang, N. Sun, H. Chen, and Y. Fang, ‘Neural Network-Based Adaptive Antiswing Control of an Underactuated Ship-Mounted Crane With Roll Motions and Input Dead Zones’, IEEE Trans Neural Netw Learn Syst, vol. 31, no. 3, pp. 901–914, Mar. 2020, doi: 10.1109/TNNLS.2019.2910580.

[6] G. P. Utomo, H. T. Wibowo, and M. A. Budiyo, ‘Stability analysis of fast ship design using flat surface hull at the fully loaded fuel tank condition’, 2021, p. 030010. doi: 10.1063/5.0063472.

[7] D. F. de C. e Silva, F. G. T. de Menezes, D. Schmidt, and P. C. de Mello, ‘Slamming Effects on FPSO Balconies: Numerical and Experimental Analysis of Alternative Configurations for Impact Attenuation’, in Volume 5: Ocean Engineering, American Society of Mechanical Engineers, Jun. 2023. doi: 10.1115/OMAE2023-105066.

[8] X. Li, Z. Yang, P. Guo, and J. Cheng, ‘An Intelligent Transient Stability Assessment Framework With Continual Learning Ability’, IEEE Trans Industr Inform, vol. 17, no. 12, pp. 8131–8141, Dec. 2021, doi: 10.1109/TII.2021.3064052.

[9] S. Fang et al., ‘Experimental study on human evacuation onboard passenger ships considering heeling angle and opposite directions’, Ocean Engineering, vol. 308, p. 118256, Sep. 2024, doi: 10.1016/j.oceaneng.2024.118256.

[10] Q. Liu, R. Zhang, S. Sun, and J. Zhang, ‘Aerodynamic Load Variation and Wind-Induced Vibration Analysis of Tower Cranes Under Full Wind Angles’, The International Journal of Acoustics and Vibration, vol. 29, no. 2, pp. 101–115, Jun. 2024, doi: 10.20855/ijav.2024.29.22016.

[11] E. Buzilă and M. Greti-Manea, ‘Stability for a parallelepipedal crane using auto-ship soft-ware’, Analele Universității ‘Dunărea de Jos’ din Galați, Fascicula XI, Construcții navale/ Annals of ‘Dunărea de Jos’ of Galati, Fascicle XI, Shipbuilding, vol. 47, pp. 123–134, Dec. 2024, doi: 10.35219/AnnUgalShipBuilding/2024.47.15.

[12] M. Faiz, Murdjito, R. W. Prastianto, E. B. Djatmiko, S. Nugroho, and Y. B. Hadasa, ‘Intact stability analysis of crane barge due to loading orientation effect during heavy lifting operation’, IOP Conf Ser Earth Environ Sci, vol. 1298, no. 1, p. 012020, Feb. 2024, doi: 10.1088/1755-1315/1298/1/012020.

[13] A. Rybicka et al., ‘The Impact of a Simplified Hydrostatic Bypass Flow Technique on Error Detection during Surgical Limb Revascularization’, J Clin Med, vol. 9, no. 4, p. 1079, Apr. 2020, doi: 10.3390/jcm9041079.

[14] U. Abbas, S. Khalid, Z. Riaz, A. Zubair, and H. Khalid, ‘Development of a Large Angle Stability Tool For The Ships and Boats’, in 2021 International Bhurban Conference on Applied Sciences and Technologies (IBCAST), IEEE, Jan. 2021, pp. 873–880. doi: 10.1109/IBCAST51254.2021.9393237.

[15] E. Miletić, L. Radić, S. Letinić, and A. Turk, ‘Seaworthiness and Stability Analysis of a Pontoon for Holiday House’, Journal of Maritime & Transportation Science, vol. Special edition 4, no. 4, pp. 305–321, Jun. 2022, doi: 10.18048/2022.04.22.

[16] A. Lamei, S. Li, M. Hayatdavoodi, and H. R. Riggs, ‘Wave-Current Interaction With Floating Objects With Square and Circular Waterplane Areas’, in Volume 5: Ocean Engineering, American Society of Mechanical Engineers, Jun. 2023. doi: 10.1115/OMAE2023-105065.

[17] L. Wang, S. Liao, S. Wang, B. Jia, J. Yin, and R. Li, ‘Real-time prediction of metacentric height of ro-ro passenger ships in Qiongzhou strait based on improved RBF neural network’, Ocean Engineering, vol. 312, p. 119067, Nov. 2024, doi: 10.1016/j.oceaneng.2024.119067.

[18] S. Song, D. Kim, and S. Dai, ‘CFD investigation into the effect of GM variations on ship manoeuvring characteristics’, Ocean Engineering, vol. 291, p. 116472, Jan. 2024, doi: 10.1016/j.oceaneng.2023.116472.

[19] N. Petacco and P. Gualeni, ‘IMO Second Generation Intact Stability Criteria: General Overview and Focus on Operational

- Measures', J Mar Sci Eng, vol. 8, no. 7, p. 494, Jul. 2020, doi: 10.3390/jmse8070494.
- [20] U. Abbas, S. Khalid, Z. Riaz, A. Zubair, and H. Khalid, 'Development of a Large Angle Stability Tool For The Ships and Boats', in 2021 International Bhurban Conference on Applied Sciences and Technologies (IBCAST), IEEE, Jan. 2021, pp. 873–880. doi: 10.1109/IBCAST51254.2021.9393237.
- [21] Q. Zhou, Y. Liu, Y. Xie, and X. Zhang, 'ANALYSIS ON ANTI-OVERTURNING STABILITY OF A TRUCK CRANE BASED ON ZERO MOMENT POINT THEORY', Dyna (Medellin), vol. 97, no. 3, pp. 281–287, May 2022, doi: 10.6036/10484.
- [22] A. N. Himaya et al., 'Effect of the loading conditions on the maneuverability of a container ship', Ocean Engineering, vol. 247, p. 109964, Mar. 2022, doi: 10.1016/j.oceaneng.2021.109964.
- [23] A. D. E. Anggriani, S. Baso, L. Bochary, Rosmani, and M. Hasbullah, 'Intact Stability Analysis of a Container Ship Due to Containers Stowage on Deck', IOP Conf Ser Earth Environ Sci, vol. 972, no. 1, p. 012047, Jan. 2022, doi: 10.1088/1755-1315/972/1/012047.
- [24] Y. Jiang, M. Wang, J. Bai, Y. Sun, and J. Li, 'Effects of outrigger configuration on trimaran stability in longitudinal waves', Ocean Engineering, vol. 280, p. 114500, Jul. 2023, doi: 10.1016/j.oceaneng.2023.114500.
- [25] G. Xing, Y. Ma, S. Chen, F. Wang, J. Zhang, and Y. Xing, 'The effects of radius and longitudinal slope of extra-long freeway spiral tunnels on driving behavior: A practical engineering design case', Tunnelling and Underground Space Technology, vol. 152, p. 105967, Oct. 2024, doi: 10.1016/j.tust.2024.105967.
- [26] Z. Cai, M. T. Herath, L. P. Djukic, D. C. Rodgers, and G. M. K. Pearce, 'Prediction of fluid surge in partially-filled clean-bore and transverse baffled tanks of multiple designs under the United Nations Model Regulations', Ocean Engineering, vol. 267, p. 113310, Jan. 2023, doi: 10.1016/j.oceaneng.2022.113310.